Hindawi Publishing Corporation
International Journal of Photoenergy
Volume 2016, Article ID 4970256, 8 pages
http://dx.doi.org/10.1155/2016/4970256

Research Article

Optical Simulation and Experimental Verification of a Fresnel Solar Concentrator with a New Hybrid Second Optical Element

Guiqiang Li[1] and Yi Jin[2]

[1]*Department of Thermal Science and Energy Engineering, University of Science and Technology of China, 96 Jinzhai Road, Hefei City 230026, China*
[2]*Department of Precision Machinery and Precision Instrumentation, University of Science and Technology of China, Hefei, Anhui, China*

Correspondence should be addressed to Guiqiang Li; ligq@mail.ustc.edu.cn and Yi Jin; jinyi08@ustc.edu.cn

Received 16 June 2016; Revised 6 September 2016; Accepted 20 October 2016

Academic Editor: Alessandro Burgio

Fresnel solar concentrator is one of the most common solar concentrators in solar applications. For high Fresnel concentrating PV or PV/T systems, the second optical element (SOE) is the key component for the high optical efficiency at a wider deflection angle, which is important for overcoming unavoidable errors from the tacking system, the Fresnel lens processing and installment technology, and so forth. In this paper, a new hybrid SOE was designed to match the Fresnel solar concentrator with the concentration ratio of 1090x. The ray-tracing technology was employed to indicate the optical properties. The simulation outcome showed that the Fresnel solar concentrator with the new hybrid SOE has a wider deflection angle scope with the high optical efficiency. Furthermore, the flux distribution with different deviation angles was also analyzed. In addition, the experiment of the Fresnel solar concentrator with the hybrid SOE under outdoor condition was carried out. The verifications from the electrical and thermal outputs were all made to analyze the optical efficiency comprehensively. The optical efficiency resulting from the experiment is found to be consistent with that from the simulation.

1. Introduction

Nowadays Fresnel solar concentrator is one of the most common solar concentrators in solar applications due to its excellent optical properties. In comparison to the parabolic dish, the Fresnel solar concentrator has a convenience for installation of PV and there is also no shading on PV. Kerzmann and Schaefer [1] simulated a linear concentrating photovoltaic system with an active cooling system. Chemisana et al. [2] conducted an experimental investigation of a Fresnel-transmission PVT concentrator for building-façade integration. Ryu et al. [3] proposed a new configuration of solar concentration optics utilizing modularly faceted Fresnel lenses to achieve a uniform intensity on the absorber plane with a moderate concentration ratio. Wu et al. [4] performed an extensive indoor experimental characterisation program to investigate the heat loss from a point focus Fresnel lens PV concentrator with a concentration ratio of 100x. Hussain and Lee [5] conducted a parametric study of a Fresnel solar concentrating photovoltaic cogeneration system with an attached thermal storage tank.

However for a high concentration Fresnel solar concentrator, the second optical element (SOE) is usually needed in actual applications because of many inevitable errors. Firstly, the Fresnel solar concentrator is restricted by the machining accuracy, which can lead to many sunrays escaping out from the absorber. Secondly, the sun-tracking system usually raises a certain error, which is different from the ideal design. Thirdly, the sunlight is the full-spectral light, which is easy to generate the dispersion phenomenon from the Fresnel lens. SOE can increase the acceptance angle and accept more sunlight for the reduction of focal aberrations. Additionally, the SOE usually can increase the concentration ratio of the whole optical system and homogenize the flux distribution on PV cell. During the study on characterization of the flux distribution and spectrum in concentrating photovoltaic

systems, Victoria et al. [6] found that adding an SOE to a Fresnel lens significantly reduces the nonuniformities and improves performance of the system.

Currently, the common SOE has two types, reflective SOE and solid lens SOE, which rely on the specular reflection function and lens refraction and total internal reflection functions, respectively. Renzi et al. [7] analyzed the performance of two 3.5 kWp CPV systems with geometrical concentration ratio of 476x and a reflective SOE. Lee and Lin [8] proposed a high-efficiency concentrated optical module with a parabolic second optical element. Benítez et al. [9] developed a Köhler-based CPV optical device with a flat Fresnel lens as the Primary Optical Element (POE) and a single refractive surface as the SOE. Terao et al. [10] presented a novel nonimaging optics design for a flat-plate concentrator PV power system with aspheric and total internal reflective SOE. Baig et al. [11] analyzed the edges feature of a total internal reflective SOE for a Fresnel solar concentrating PV system.

In this paper, based on the Fresnel solar concentrator of 1090x, the hybrid SOE was designed to improve the optical performance. The optical software *Lighttools* was employed to simulate the optical properties at different deviation angles. The optical efficiency and flux distribution were all analyzed to demonstrate the performance. In addition, the experiment of the Fresnel solar concentrator with the hybrid SOE under outdoor condition was carried out. The verifications from the electrical and thermal outputs were all made to analyze the optical efficiency comprehensively. The experimental results indicated that the optical efficiency is in well agreement with that in the simulation.

2. Structure

The Fresnel solar concentrator consists of series of prisms. According to the refraction law, the curves of prisms can be easily obtained. Huang et al. [12] presented a Fresnel lens design for CPV. N. Yeh and P. Yeh [13] analyzed a point-focused, nonimaging Fresnel lens concentration profile and established parameters in detail. The curves of prisms of a flat Fresnel solar concentrator can easily be attained, as shown in Figure 1.

Based on the geometrical principle, the following values of parameters can be obtained:

$$\alpha = i, \qquad r = \alpha + \beta, \tag{1}$$

$$\tan\beta = \tan(j-\alpha) = \frac{l}{f}. \tag{2}$$

Based on the refraction law,

$$n = \frac{\sin j}{\sin i} = \frac{\sin(\alpha+\beta)}{\sin\alpha} = \frac{\sin\alpha\cos\beta + \cos\alpha\sin\beta}{\sin\alpha} = \cos\beta + \frac{\sin\beta}{\tan\alpha}. \tag{3}$$

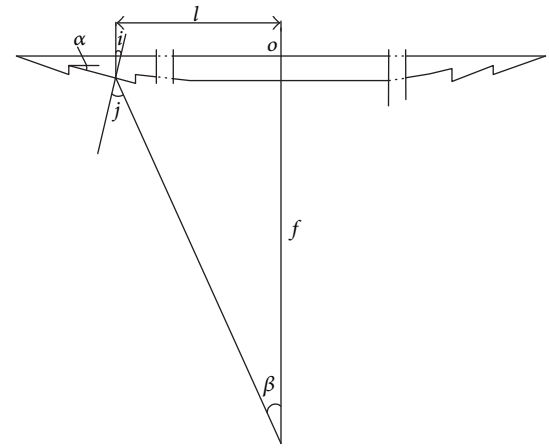

Figure 1: Schematic diagram of a flat Fresnel solar concentrator.

Combiningg (1) and (3),

$$\tan\alpha = \frac{\sin(j-\alpha)}{n-\cos(j-\alpha)} = \frac{\tan(j-\alpha)}{n/\cos(j-\alpha)-1}. \tag{4}$$

According to the Pythagorean identity,

$$\cos(j-\alpha) = \sqrt{\frac{1}{\tan^2(j-\alpha)+1}} = \frac{f}{\sqrt{l^2+f^2}}. \tag{5}$$

Substitute (2) and (5) into (4):

$$\alpha = \arctan\left(\frac{l/f}{n\sqrt{1+(l/f)^2}-1}\right). \tag{6}$$

From (6), the curves of the prisms can be calculated.

For the second optical element, there are many different designs. The specular reflective SOE and total internal reflective SOE are common in the application [7, 14, 15]. In this paper, the hybrid SOE is designed for the Fresnel solar concentrator, which consisted of the reflective element and the solid lens element. The cross sections of reflective element and solid lens element are all symmetrical trapezoids (Figure 2), and the solid lens element is located in the inner bottom side of the reflective element. The water cooling system is employed to take the heat away from the PV. The dimensions of different parts are shown in Table 1.

3. Ray-Tracing Analysis

Exporting the concentrating system model built by *Solidworks* in IGES format to optical software *Lighttools* was used to simulate the optical path. The inner reflection surface was defined as aluminum and its reflectivity is assumed to be 92%. The light is defined by a 0.53° convergence angle which is not a parallel beam as the sunlight's converging angle is 4.7 mrad. Figure 3 shows the schematic diagram of ray tracing at the deflection angle 0°. The deflection angle is the angle between the direction of the incident sunrays and the perpendicular

Table 1: Size parameters of the Fresnel solar concentrator with the hybrid SOE.

Parameter	Value
Fresnel lens area (m^2)	$0.33 * 0.33$
Top aperture area of reflective element (m^2)	$0.044 * 0.044$
Bottom aperture area of reflective element (m^2)	$0.01 * 0.01$
Top surface area of solid lens element (m^2)	$0.014 * 0.014$
Bottom surface area of solid lens element (m^2)	$0.009 * 0.009$

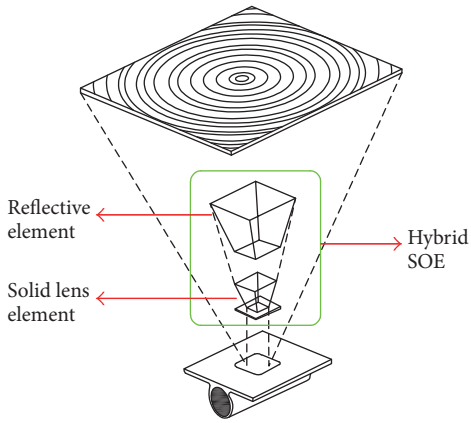

Figure 2: Schematic diagram of a Fresnel solar concentrator with the hybrid SOE.

to the aperture of the solar concentrator. Firstly, the sunlight will be concentrated by the flat Fresnel lens. Secondly, many sunlight rays can be reflected by the reflective element into the solid lens element; then we research the top surface of the PV through the refraction and total internal reflection function of lens element. Other sunlight rays can pass through the lens element directly to reach the top surface of PV.

3.1. Optical Efficiency. Ten thousand direct sun light rays across the Fresnel solar concentrator were traced at different deflection angles. The optical efficiency can be obtained as follows:

$$\eta_{opt} = \frac{\phi_{ab}}{\phi_{tot}}, \tag{7}$$

where ϕ_{ab} is the radiation received by the absorber and ϕ_{tot} is the total radiation emitted by the light source.

Through the software simulation, the optical efficiency can be attained (Figure 4). It can be seen that the optical efficiency is above 90.0% for deflection angles smaller than 0.5°. The curve of the optical efficiency shows a declining trend with the increase in deflection angle and when the deflection angle is larger than 0.5°, the optical efficiency cannot sustain a high value. However, when the deflection angle is between 0.6° and 0.7°, the optical efficiency is still between 85.0% and 90.0%.

3.2. Flux Distribution. The simulation was performed under the standard solar irradiation of 1000 W/m^2 and the spectral

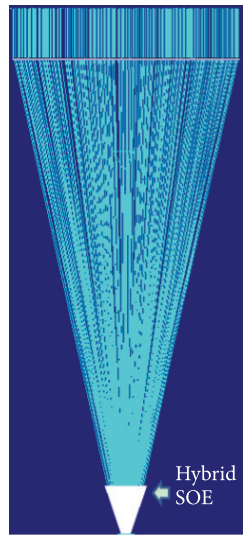

Figure 3: Schematic diagram of ray tracing at deflection angle 0°.

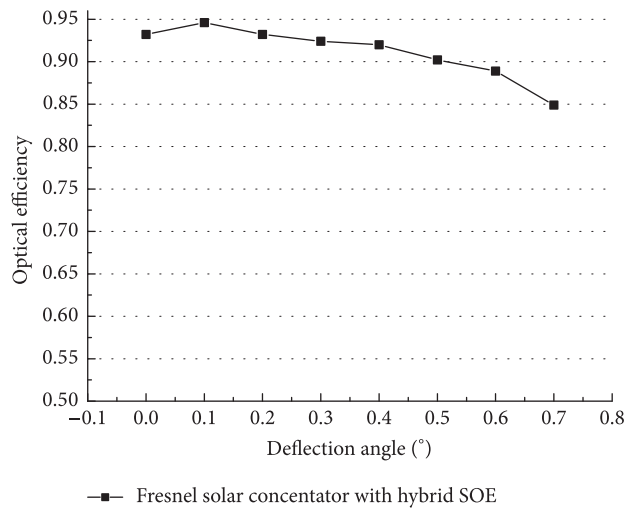

Figure 4: Optical efficiency with different deflection angles.

wavelength is between 300 and 1800 nm. It can be seen from Figure 5 that when the deflection angle is 0°, the highest flux distribution is below $2 * 10^6$ W/m^2 and the position is on the center of the PV. Approximately 80% area of PV owns the flux density of above 10^6 W/m^2. Therefore, the flux on PV at this deflection angle has a relatively uniform distribution.

When deflection angles are 0.1° and 0.2°, the highest fluxes are all on the left section of the PV top surface. With the increase of the deflection angle, the highest flux furtherly moves to the left position (Figure 6).

Figure 7 shows the flux distribution at a larger deflection angle scope between 0.3° and 0.6°. The tendency of the flux distribution shows that the flux on left section is higher than that at the right section. Actually, this deflection angle scope is larger than the error from the tracking system (0.3°), but considering the errors from the processing and installment, and so forth, the actual flux distribution may

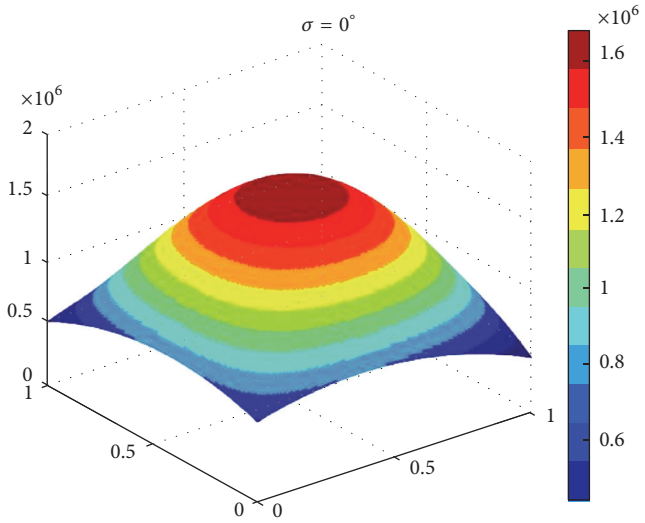

Figure 5: Flux distribution at deflection angle of 0°.

be more complex than the simulation. Therefore, the high optical system needs a larger deflection angle scope (>0.3°). From the simulation, the basic orders of magnitude of the flux distribution may be identified, which will give the reference for the evaluation of the actual system operation.

4. Experimental Verification

4.1. Experiment Setup. The Fresnel solar concentrator is integrated with high-efficiency InGaP/GaAs/Ge triple-junction solar cells, whose electrical efficiency is 31.4% (AM1.5D, 25°C) under one sun. The Fresnel solar concentrating PV module consists of 15 PV/T components and 15 point-focus Fresnel lenses with hybrid SOE as shown in Figure 8(a). One of the 15 point-focus Fresnel lenses was tested in this experiment. The area of each Fresnel lens is $330.0 * 330.0\,\text{mm}^2$, and the size of each solar cell is $10 * 10\,\text{mm}^2$, which is consistent with the one in the simulation. The solar cell is pasted on the bottom surface of the solid lens element, as shown in Figure 8(b). A two-axis tracking system is employed. A couple of light sensors are installed on the tilt axis to feed back the location of the sun to the tracking control system; thus it maintains the angle of deflection for the Fresnel solar concentrator within a range of 0.3°. In the test system, the temperature is measured by T-type thermocouples. The direct radiation is measured by a normal incidence pyranometer. An inverter is used to measure and record the electrical power output. The components of the test equipment are shown in Table 2.

4.2. Error Analysis. According to the theory of error propagation, the relative error (RE) of the dependent variable y can be calculated as follows:

$$\text{RE} = \frac{dy}{y} = \frac{\partial f}{\partial x_1}\frac{dx_1}{y} + \frac{\partial f}{\partial x_2}\frac{dx_2}{y} + \cdots + \frac{\partial f}{\partial x_n}\frac{dx_n}{y}, \quad y = f(x_1, x_2, \ldots, x_n), \tag{8}$$

Table 2: The components of the test equipment.

Equipment (specification)	Accuracy
Thermocouple (T-type)	±0.2°C
Normal incidence pyranometer (TBS 2-2)	2%
Inverter (Guanya GSG-100KTT-TV)	3%
Flowmeter (LXS-40E)	2%
Data logger (Agilent 34970A (USA))	—

Table 3: Experimental RME of the variables.

Variable	T	G	η_{pv}	η_{th}
RME	0.063%	2.0%	3.0%	19.7%

where x_i $(i = 1, \ldots, n)$ is the variable of the dependent variable y. $\partial f/\partial x$ is the error transferring coefficient of the variables.

The experimental relative mean error (RME) during the test period can be expressed as

$$\text{RME} = \frac{\sum_1^N |\text{RE}|}{N}. \tag{9}$$

According to (8)~(9), the RMEs of all variables (temperature, solar irradiation, PV efficiency, and thermal efficiency) were all calculated and the results were given in Table 3.

4.3. Experiment Analysis

4.3.1. Verification Based on the Electrical Output. The experiment was made in a sunny day. The water took the heat from the PV to harvest the thermal energy. The ambient parameters and test outcomes were shown in Table 4.

For the solar concentrating PV, the fill factor (FF) drops slightly under concentrating condition because of the nonuniform flux distribution [16–18].

The FF can be obtained by

$$\text{FF} = \frac{P_{\max}}{I_{sc} \cdot V_{oc}}, \tag{10}$$

where $P_{\max}$ is the maximal power output; I_{sc} is the short-circuit current; and V_{oc} is the open-circuit voltage.

The variation scopes of FF between 25°C and 50°C are between 0.828 and 0.844, as shown in Figure 9. Therefore, it can be concluded that the flux distribution on PV is relatively uniform during the system operation. It can also be inferred that the Fresnel solar concentrating PV with the hybrid SOE can work well under the current tracking system, installment, and processing technology.

For the system, the electrical efficiency can be expressed as

$$\eta_{pv} = \eta_{opt} \cdot \eta_{cell}, \tag{11}$$

where η_{pv} is the system electrical efficiency; η_{opt} is the optical efficiency; and η_{cell} is the solar cell electrical efficiency.

The PV efficiency at different operation temperature can be expressed as [19]

$$\eta_{cell} = \eta_r \left(1 - B_r \left(T_{pv} - T_r\right)\right), \tag{12}$$

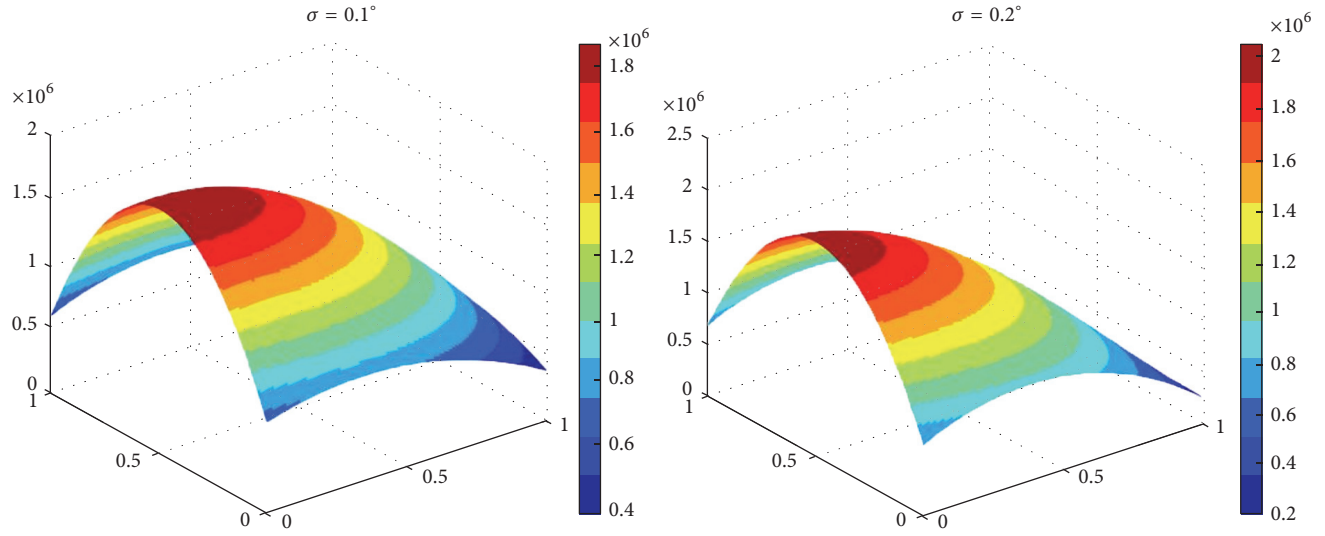

FIGURE 6: Flux distribution at deflection angles of 0.1° and 0.2°.

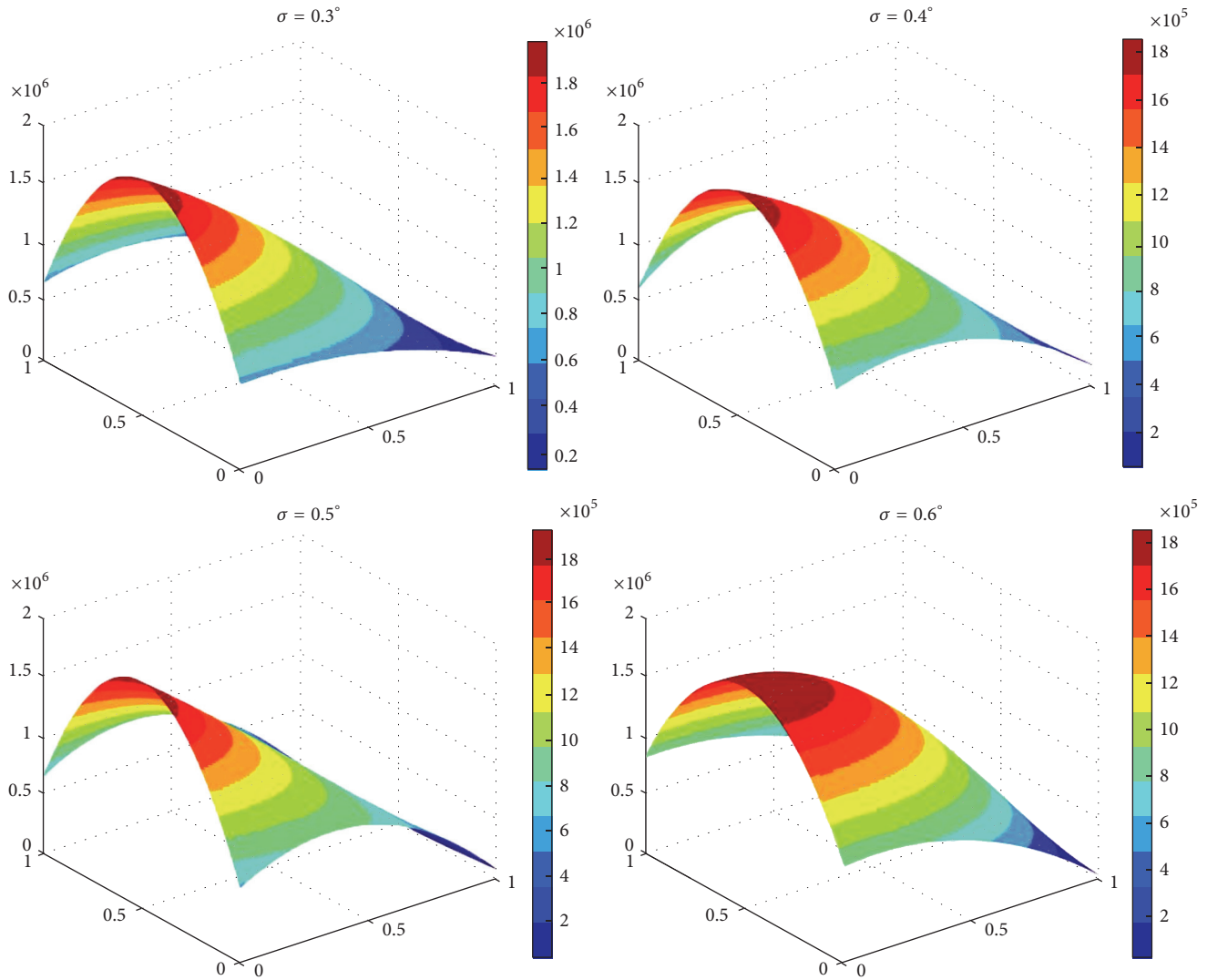

FIGURE 7: Flux distribution at deflection angles of 0.3°, 0.4°, 0.5°, and 0.6°.

Table 4: Relative parameters at different PV temperatures.

Parameters	T_{cell} = 25°C	T_{cell} = 30°C	T_{cell} = 35°C	T_{cell} = 40°C	T_{cell} = 45°C	T_{cell} = 50°C
Ambient temperature (°C)	16.5	17.1	16.4	16.6	18.6	18.4
Direct irradiation (W/m^2)	663.3	677.9	710.7	702.9	709.2	683.3
Open-circuit voltage (V)	3.03	3.02	3.01	2.99	2.97	2.95
Short-circuit current (A)	8.20	8.29	8.63	8.50	8.51	8.28
Voltage on maximum power point (V)	2.7	2.6	2.6	2.6	2.6	2.6
Current on maximum power point (A)	7.7	8.0	8.4	8.2	8.2	8.0
Maximum out power (W)	20.5	21.1	21.9	21.4	21.1	20.5

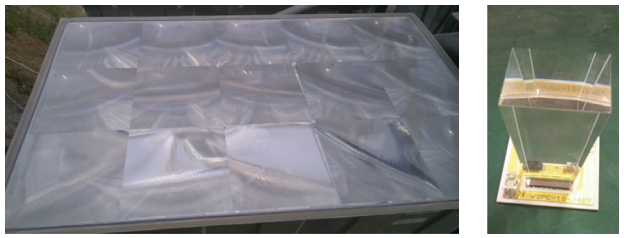

(a) (b)

Figure 8: Photo of Fresnel solar concentrators.

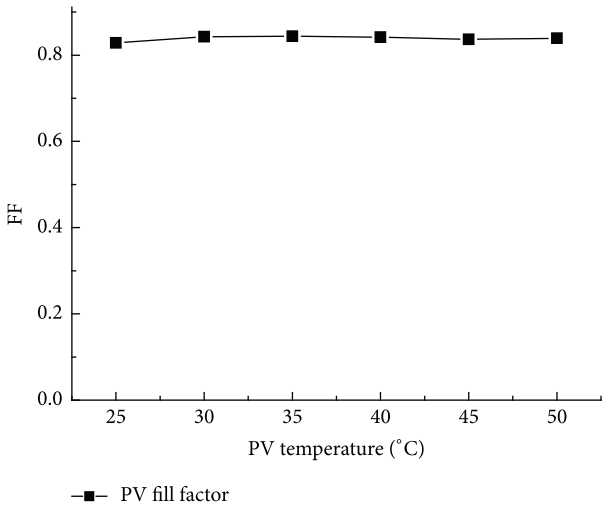

Figure 9: Fill factor of PV on different PV temperatures.

where η_r is the reference solar cell efficiency at the reference operating temperature; T_r = 298.15 K; B_r = 0.002 K^{-1}; and T_{pv} is the actual TV temperature.

The system electrical efficiency can also be attained by

$$\eta_{pv} = \frac{P_{max}}{C \cdot G_{dir} \cdot A_{cell}} = \frac{I_m \cdot V_m}{C \cdot G_{dir} \cdot A_{cell}}. \quad (13)$$

The electrical efficiency on different PV temperature was shown in Figure 10. With the increase of PV temperature, the electrical efficiency has a downward trend. But the electrical efficiency is still above 27.5%, which indicates that the Fresnel solar concentrator has a high electrical efficiency.

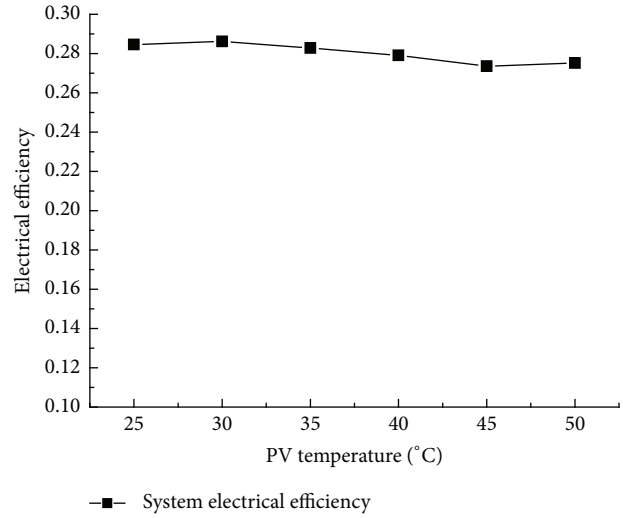

Figure 10: Electrical efficiency on different PV temperatures.

Combining (11) and (13), the optical efficiency of this high solar concentrator can be obtained, as expressed in (14), and the curve of optical efficiency is shown in Figure 11.

$$\eta_{opt} = \frac{I_m \cdot V_m}{C \cdot G_{dir} \cdot A_{cell} \cdot \eta_r \left(1 - B_r \left(T_{pv} - T_r\right)\right)}. \quad (14)$$

The optical efficiencies resulting from the experiment are between 90.7% and 92.3%, which are close to the simulated values. Therefore, the design of the Fresnel solar concentrator with hybrid SOE is reasonable and the whole optical system has a high optical efficiency for the high concentrating PV/T application.

4.3.2. Verification Based on the Thermal Output. In order to further illustrate the optical efficiency, the thermal efficiency can also be analyzed. Thirty Fresnel solar concentrating PV/T were connected and the water was circulated between the series of solar concentrators and the storage tank having 70 L volume.

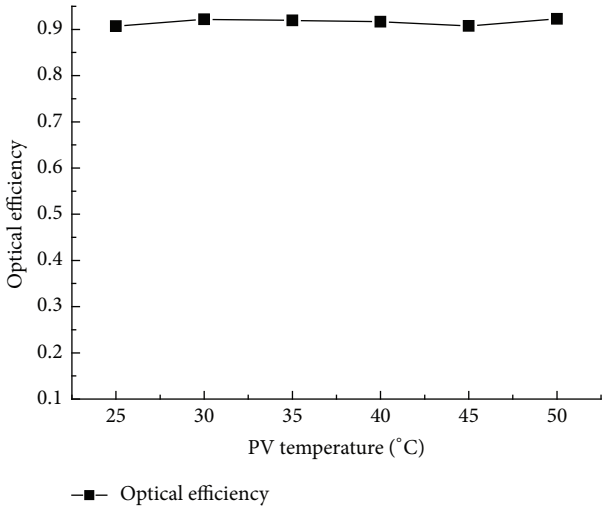

Figure 11: Optical efficiency on different PV temperatures.

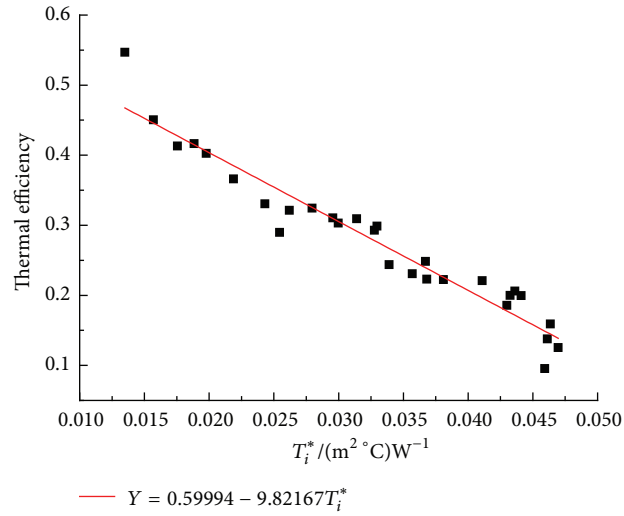

Figure 12: Thermal efficiency fit curve of the experimental results.

The thermal efficiency at any given time can be calculated as follows:

$$\eta_{\text{th}} = \frac{q_{\text{sys}}}{C \cdot G_{\text{dir}} \cdot A_{\text{cell}}},$$
$$q_{\text{sys}} = m_{\text{water}} \cdot c_{\text{water}} \cdot \frac{d\overline{T}}{dt}, \tag{15}$$

where $\overline{T}$ is the average water temperature in the tank.

The thermal efficiency can also be expressed by

$$\eta_{\text{th}} = \alpha - UT_i^* = \alpha - U\frac{T_i - \overline{T}_a}{\overline{G}}. \tag{16}$$

The system thermal efficiencies of series of experimental data were fitted to a linear function to correspond to mutual relationships among the variables, as shown in Figure 12.

The thermal efficiency equation is as follows:

$$\eta_{\text{th}} = 0.5999 - 9.8217\frac{T_i - \overline{T}_a}{\overline{G}}. \tag{17}$$

The thermal efficiency intercept is about 0.6. Combining with the electrical efficiency of approximately 0.3, the overall efficiency is above 0.9. In this situation, the water temperature is equal to the ambient temperature; thus the thermal loss of the system is less. Consequently, the greatest loss is the optical loss, which is lower than 0.1. From this point of view, the optical efficiency is slightly higher than 90.0%, which is also verified in the thermal performance.

5. Conclusion

This paper presents the optical performance of a Fresnel solar concentrator with a new hybrid SOE, which includes the reflective element and the solid lens element.

The ray tracing was employed in the simulation on the optical properties. The simulation results indicated that the optical efficiencies were all above 90.0% within the deflection angles of 0°–0.5°, and at the deflection angles of 0.6° and 0.7°, the optical efficiencies were still above 85.0%. At the same time, the flux distribution at different deflection angles was also demonstrated and analyzed.

The preliminary experiment was also conducted to verify the simulation results. Based on the output, the fill factor, the system electrical efficiency, and the thermal efficiency were all analyzed, which indicated that the Fresnel solar concentrating PV with the new hybrid SOE has a high output performance. Through the calculation, the optical efficiency was also attained, and it is still larger than 90.0% during operation, which agreed well with that in the simulation.

Therefore, the design of the SOE for the Fresnel solar concentrator is reasonable, and the high solar concentrating system can overcome errors of processing, installment, tracking system, and so on to keep a high output performance in actual application.

Competing Interests

The authors declare that they have no competing interests.

Acknowledgments

The study was sponsored by the National Science Foundation of China (Grant nos. 51408578, 51605464, and 51611130195) and Anhui Provincial Natural Science Foundation (1508085QE96). The authors would like to thank Professor Zheng Hongfei (School of Mechanical Engineering, Beijing Institute of Technology, China) for his assistance in the software simulation.

References

[1] T. Kerzmann and L. Schaefer, "System simulation of a linear concentrating photovoltaic system with an active cooling system," *Renewable Energy*, vol. 41, pp. 254–261, 2012.

[2] D. Chemisana, J. I. Rosell, A. Riverola, and C. Lamnatou, "Experimental performance of a Fresnel-transmission PVT concentrator for building-façade integration," *Renewable Energy*, vol. 85, pp. 564–572, 2016.

[3] K. Ryu, J.-G. Rhee, K.-M. Park, and J. Kim, "Concept and design of modular Fresnel lenses for concentration solar PV system," *Solar Energy*, vol. 80, no. 12, pp. 1580–1587, 2006.

[4] Y. Wu, P. Eames, T. Mallick, and M. Sabry, "Experimental characterisation of a Fresnel lens photovoltaic concentrating system," *Solar Energy*, vol. 86, no. 1, pp. 430–440, 2012.

[5] M. I. Hussain and G. H. Lee, "Parametric performance analysis of a concentrated photovoltaic co-generation system equipped with a thermal storage tank," *Energy Conversion and Management*, vol. 92, pp. 215–222, 2015.

[6] M. Victoria, R. Herrero, C. Domínguez, I. Antõn, S. Askins, and G. Sala, "Characterization of the spatial distribution of irradiance and spectrum in concentrating photovoltaic systems and their effect on multi-junction solar cells," *Progress in Photovoltaics: Research and Applications*, vol. 21, no. 3, pp. 308–318, 2013.

[7] M. Renzi, L. Egidi, and G. Comodi, "Performance analysis of two 3.5 kWp CPV systems under real operating conditions," *Applied Energy*, vol. 160, pp. 687–696, 2015.

[8] C.-J. Lee and J.-F. Lin, "High-efficiency concentrated optical module," *Energy*, vol. 44, no. 1, pp. 593–603, 2012.

[9] P. Benítez, J. C. Miñano, P. Zamora et al., "High performance fresnel-based photovoltaic concentrator," *Optics Express*, vol. 18, no. 9, pp. A25–A40, 2010.

[10] A. Terao, W. P. Mulligan, S. G. Daroczi et al., "A mirror-less design for micro-concentrator modules," in *Proceedings of the 28th IEEE Photovoltaic Specialists Conference (PVSC '00)*, pp. 1416–1419, Anchorage, Alaska, USA, September 2000.

[11] H. Baig, N. Sellami, and T. K. Mallick, "Trapping light escaping from the edges of the optical element in a Concentrating Photovoltaic system," *Energy Conversion and Management*, vol. 90, pp. 238–246, 2015.

[12] H. Huang, Y. Su, Y. Gao, and S. Riffat, "Design analysis of a Fresnel lens concentrating PV cell," *International Journal of Low-Carbon Technologies*, vol. 6, no. 3, pp. 165–170, 2011.

[13] N. Yeh and P. Yeh, "Analysis of point-focused, non-imaging Fresnel lenses' concentration profile and manufacture parameters," *Renewable Energy*, vol. 85, pp. 514–523, 2016.

[14] N. Yeh, "Optical geometry approach for elliptical Fresnel lens design and chromatic aberration," *Solar Energy Materials and Solar Cells*, vol. 93, no. 8, pp. 1309–1317, 2009.

[15] A. W. Bett, C. Baur, F. Dimroth et al., "Flatcon™-modules: technology and characterisation," in *Proceddings of the 3rd World Conference on Photovoltaic Energy Conversion*, pp. 634–637, Osaka, Japan, May 2003.

[16] L. Guiqiang, P. Gang, S. Yuehong, W. Yunyun, and J. Jie, "Design and investigation of a novel lens-walled compound parabolic concentrator with air gap," *Applied Energy*, vol. 125, pp. 21–27, 2014.

[17] L. Guiqiang, P. Gang, S. Yuehong, J. Jie, and S. B. Riffat, "Experiment and simulation study on the flux distribution of lens-walled compound parabolic concentrator compared with mirror compound parabolic concentrator," *Energy*, vol. 58, pp. 398–403, 2013.

[18] G. Li, G. Pei, J. Ji, and Y. Su, "Outdoor overall performance of a novel air-gap-lens-walled compound parabolic concentrator (ALCPC) incorporated with photovoltaic/thermal system," *Applied Energy*, vol. 144, pp. 214–223, 2015.

[19] G. Li, G. Pei, J. Ji, M. Yang, Y. Su, and N. Xu, "Numerical and experimental study on a PV/T system with static miniature solar concentrator," *Solar Energy*, vol. 120, pp. 565–574, 2015.